



The Attenuation Value Within the Non-hypodense Region on Non-contrast Computed Tomography of Spontaneous Cerebral Hemorrhage: A Long-Neglected Predictor of Hematoma Expansion

OPEN ACCESS

Edited by:

Guofeng Wu,

Affiliated Hospital of Guizhou Medical University, China

Reviewed by:

Jawed Nawabi,

University Medical Center Hamburg-Eppendorf, Germany

Khalid Sawalha,

Baystate Medical Center,

United States

Qi Li,

The First Affiliated Hospital of Chongqing Medical University, China

*Correspondence:

Jian Chen

hustjichen110@163.com

Specialty section:

This article was submitted to

Stroke,

a section of the journal

Frontiers in Neurology

Received: 29 September 2021

Accepted: 08 March 2022

Published: 08 April 2022

Citation:

Chen Y, Cao D, Guo Z-Q, Ma X-L, Ou Y-B, He Y, Chen X and Chen J (2022) The Attenuation Value Within the Non-hypodense Region on Non-contrast Computed Tomography of Spontaneous Cerebral Hemorrhage: A Long-Neglected Predictor of Hematoma Expansion. *Front. Neurol.* 13:785670. doi: 10.3389/fneur.2022.785670

Yong Chen¹, Dan Cao¹, Zheng-Qian Guo¹, Xiao-Ling Ma², Yi-Bo Ou¹, Yue He¹, Xu Chen¹ and Jian Chen^{1*}

¹ Department of Neurosurgery, Tongji Hospital, Tongji Medical College, Huazhong University of Science and Technology, Wuhan, China, ² Department of Radiology, Tongji Hospital, Tongji Medical College, Huazhong University of Science and Technology, Wuhan, China

Background and Purpose: The ability of attenuation value of the non-hypodense region of hematoma in non-contrast computed tomography (NCCT) for predicting hematoma expansion (HE) remains unclear. Our purpose is to explore this relationship.

Methods: Two cohorts of patients were collected for analysis. The region where we measured hematoma attenuation values was limited to the non-hypodense region that was not adjacent to the normal brain tissue on NCCT. The critical attenuation value was derived *via* receiver operating characteristic (ROC) curve analysis in the derivation cohort and its predictive ability was validated in the validation cohort. Independent relationships between predictors, such as critical attenuation value of the non-hypodense region and HE were analyzed using the least absolute shrinkage and selection operator (LASSO) regression and multivariate logistic analysis.

Results: The results showed that the attenuation value <64 Hounsfield units (HU) was independently associated with HE [odds ratio (OR), 4.118; 95% confidential interval (CI), 1.897–9.129, $p < 0.001$] and the sensitivity, specificity, positive predictive value (PPV), negative predictive value (NPV), positive likelihood ratio (PLR), negative likelihood ratio (NLR), and area under the curve (AUC) for predicting HE were 36.11%, 81.71%, 1.97, 0.78, 44.8%, 75.7%, and 0.589, respectively.

Conclusions: Our research explored and validated the relationship between the attenuation value of the non-hypodense region of hematoma and HE. The attenuation value < 64 HU was an appropriate indicator of early HE.

Keywords: attenuation value, non-hypodense region, hematoma expansion, Hounsfield units, non-contrast computed tomography, spontaneous intracerebral hemorrhage

INTRODUCTION

Hematoma expansion (HE) occurs in approximately one-third of patients with spontaneous intracerebral hemorrhage, and it is an independent risk factor for the worsening prognosis and early death (1). Early recognition of HE is considered as one of the potential therapeutic goals to improve prognosis (2, 3). In addition to the spot sign and its density on contrast CT (4), the presence of hypodense areas within the hematoma on non-contrast computed tomography (NCCT) is an important factor in assessing the inefficient clot contraction and the instability of intracerebral hematomas with a high discriminating ability (5). However, the hypodense foci on NCCT do not always match the location of the spot sign suggestive of contrast leakage on contrast CT (6), which may be implicated in the relatively low sensitivity of the NCCT signs in predicting HE (7–9). Minimally invasive surgery appeared to reduce the poor prognosis of patients at high risk of hematoma expansion, yet this difference was not significant for reasons that cannot be ruled out due to the inability to accurately identify the actual hematoma that will undergo expansion (10). In our clinical work, we have noticed that some homogeneous hematomas dilated (>6 ml or 33% increase compared with baseline volume) without any hypodensity foci but with overall low attenuation value, some dilated heterogeneous hematomas (those with a swirl sign, black hole sign, or blend sign) with relatively low attenuation value within the non-hypodense region, while some non-dilated heterogeneous hematomas have relatively high attenuation values within the non-hypodense region (Figure 1), prompting us to wonder that whether low attenuation value of the non-hypodense region is a risk factor for HE. Therefore, this study aims to investigate the clinical significance of the attenuation value within the non-hypodense region for predicting HE.

MATERIALS AND METHODS

Patients

Patients with spontaneous intracerebral hemorrhage admitted to our three hospital branches from January 2013 to June 2021 were selected for this retrospective study. Inclusion criteria for eligible patients were (1) the first NCCT examination was performed within 6 h after onset and (2) one or more NCCT re-examinations were performed within 72 h after onset. Exclusion criteria were (1) patient age <18 years old; (2) intracerebral hemorrhage secondary to arteriovenous malformation, aneurysm, trauma, tumor, Moya-Moya disease, or other diseases; (3) multiple cerebral hemorrhages or primary ventricular hemorrhage; (4) any form of neurosurgery performed before the first NCCT re-examination; (5) patients with axial layers <3 on the first NCCT scan (aiming to eliminate partial volume effects when extracting hematoma attenuation values); and (6) baseline hematoma volume <1 ml.

Abbreviations: NCCT, non-contrast computed tomography; HE, hematoma expansion; ROC, receiver operating characteristic; LASSO, least absolute shrinkage and selection operator; HU, Hounsfield units; PPV, positive predictive value; NPV, negative predictive value; PLR, positive likelihood ratio; NLR, negative likelihood ratio; AUC, area under the curve; IQR, interquartile range.

Derivation Cohort

Eligible patients admitted in the main hospital site from January 2013 to August 2015 were included as a derivation cohort according to the inclusion and exclusion criteria described above. Attenuation value within the non-hypodense region of the hematoma was examined retrospectively for suitability to predict HE, and a cutoff value was determined by an ROC analysis based on the maximum Youden index.

Validation Cohort

Patients admitted in the main hospital site between September 2015 and June 2021 ($n = 119$) and two other branch sites (October 2015 to June 2021, $n = 70$; November 2017 to June 2021, $n = 58$) who met the above criteria were included as a validation cohort. A validating analysis was performed to investigate whether a critical attenuation value of the non-hypodense region could predict HE in this cohort. The studies involving human participants were reviewed and approved by the local ethics committee. Written informed consent was not required for this study due to the de-identified retrospective data.

Clinical Information

Clinical information for each patient is collected from the electronic medical records, such as demographic characteristics, medical history, physical examination items, and potentially relevant laboratory tests at the time of admission (Table 1).

Imaging Characteristics

Non-contrast computed tomography images of the patients were obtained by standard clinical protocols (120 kV, axial section 5–7.5 mm thick). Baseline hematoma volume was calculated *via* the Tada formula $ABC/2$. The NCCT image data with DICOM format of each patient were used to measure the attenuation value of the non-hypodense region of the hematoma in the Picture Archiving and Communication System (PACS). The non-hypodense region was restricted to any layer within the highest density region of the heterogeneous hematoma as well as the core region of the homogeneous hematomas. When the standard deviation of the mean HU value in the region of interest of the non-hyperdense region is ≤ 6 , this part of the hematoma is considered to be homogeneous. The layer used to measure the attenuation value was limited to the core axial section of the hematoma, and the upper and lower layers adjacent to the normal brain tissue were not used for measurement (Figure 2). The attenuation value of the hematoma was assessed independently by two experienced raters (YC and DC) who were unaware of the outcome of patient. The midline shift distance was defined as the maximum lateral vertical displacement distance of brain tissue structures in the horizontal plane from the mid-axis sagittal plane of the NCCT scan. The definitions of irregular sign, satellite sign, island sign, swirl sign, black hole sign, and blend sign were conformed to the standards that were proposed by Andrea Morotti et al. (11). HE or dilated hematoma was defined as a >33% or >6 ml increase of hematoma volume or new intraventricular hematoma development on the NCCT re-examination (Figure 3) (12).

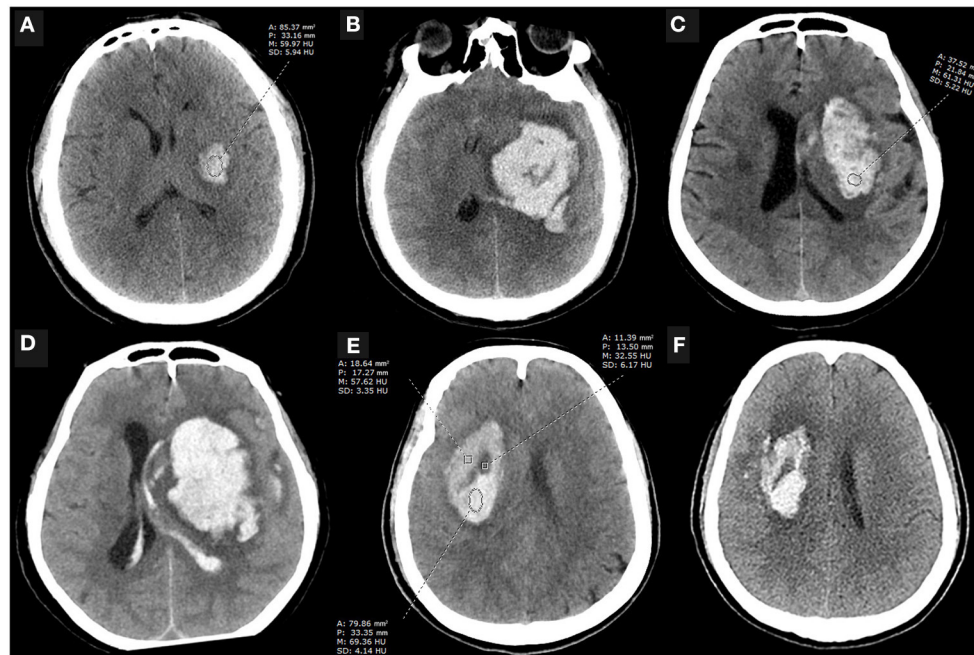


FIGURE 1 | Case examples. **(A,B)** An initial NCCT scan performed 3.5 h after the onset of symptoms showed a small, regular shape hematoma with an attenuation value of 61.72 HU at the internal capsule, which enlarged 10 h later. The patient eventually died. **(C,D)** An NCCT scan performed 0.5 h after symptom onset showed a basal ganglia hematoma that was heterogeneous with an attenuation value of 63.86 HU within the non-hypodense region and appeared significantly expansion 12 h later. **(E,F)** NCCT scan performed 1 h after onset showed a heterogeneous basal ganglia hematoma with an attenuation value of more than 64 HU in the non-hypodense region, and the patient did not present with HE despite the presence of the black hole sign on the initial NCCT examination. A, area; P, perimeter; M, mean; SD, standard deviance; HU, Hounsfield units; NCCT, non-contrast computed tomography.

Statistical Analysis

Statistical analyses were performed with R software (version 4.0.5, <http://www.Rproject.org>) and the SPSS package (version 24.0, IBM Corporation, Armonk, NY). Categorical variables were expressed as percentages (%) and continuous variables were expressed as means [\pm standard deviation (SD)] or medians (interquartile range, IQR). Cohen's κ -test was used to determine inter- and intra-rater agreement referring to the NCCT signs and attenuation value level. A univariate analysis was performed using chi-square test, Fisher's exact test, two-tailed Student's *t*-test, or univariate logistic analysis, as appropriate. An ROC curve analysis with Delong's test was used to obtain cutoff for attenuation value within the non-hypodense region of the hematoma and to obtain the sensitivity, specificity, PPV, NPV, PLR, NLR, and AUC values. Considering the possible collinearity between variables, the least absolute shrinkage and selection operator (LASSO) regression was first used to screen the potential predictors of HE (13), and then variables with non-zero coefficients were further included in the multivariate model. The model was visualized using the nomogram and the discrimination and calibration of the prediction were observed by the use of Harrell's concordance index (C-index)/AUC of ROC analysis and calibration plot. The decision curve analysis and clinical impact curve analysis were used to observe the performance of the attenuation value within the non-hypodense region in the terms of improving the predictive power of

the model. A two-tailed test of $p < 0.05$ was considered statistically significant.

RESULTS

Clinical and Radiological Characteristics and Outcomes of Two Cohorts

In the primary and validation cohorts, 31 of 132 patients (23.5%) and 72 of 247 patients (29.1%) experienced HE. The median attenuation value of the non-hypodense region of hematoma was 66.2 HU [IQR, 63.1–69.3 HU] in the derivation cohort and 67.6 HU [IQR, 64.4–70.8 HU] in the validation cohort. **Supplementary Figure 1** shows the patient selection process for both cohorts. The clinical and radiological characteristics and the outcomes of two cohort patients are shown in **Table 1**.

Factors Associated With the Attenuation Value of the Non-hypodense Region of the Hematoma in the Validation Cohort

The correlation matrix heatmap for continuous variables are shown in **Supplementary Figure 2**. In homogeneous hematomas, the attenuation value within the core region was relatively low in those with HE compared with those without HE, and without a significant increasing trend over time (**Figure 4A**). In heterogeneous density hematomas, there was

TABLE 1 | Comparison of clinical and radiological characteristics and the outcome of derivation and validation cohort patients.

Variables	Derivation cohort (n = 132)	Validation cohort (n = 247)	P
Clinical characteristics			
Age, years, mean (SD)	55.0 (11.1)	57.6 (12.4)	0.039
Sex, male (%)	88 (66.7)	162 (65.6)	0.922
Hypertension (%)	81 (61.4)	171 (69.2)	0.152
Diabetes (%)	13 (9.85)	21 (8.50)	0.804
Current smoker (%)	50 (37.9)	46 (18.6)	<0.001
Current alcohol drinker (%)	36 (27.3)	42 (17.0)	0.026
Stroke history (%):			0.812
No	117 (88.6)	210 (85.0)	
Hemorrhage	6 (4.55)	17 (6.88)	
Infarction	8 (6.06)	17 (6.88)	
Hemorrhage and infarction	1 (0.76)	3 (1.21)	
Antiplatelets or anticoagulants therapy (%)	5 (3.79)	11 (4.45)	0.969
Systolic pressure on admission (mmHg), median [IQR]	162 [146; 178]	160 [144; 180]	0.807
Diastolic pressure on admission (mmHg), mean (SD)	92.4 (16.9)	92.9 (15.5)	0.795
Baseline GCS score (%):			0.519
12–15	51 (38.6)	109 (44.1)	
9–11	52 (39.4)	84 (34.0)	
3–8	29 (22.0)	54 (21.9)	
RBC count (*10 ¹² /L), median [IQR]	4.64 [4.37; 4.95]	4.62 [4.28; 5.00]	0.447
Hemoglobin (g/L), median [IQR]	140 [129; 150]	139 [129; 151]	0.475
Hematocrit (%), median [IQR]	41.6 [38.7; 43.7]	41.2 [38.7; 44.3]	0.700
MCV (fl), median [IQR]	89.1 [86.7; 91.4]	89.9 [87.0; 92.5]	0.237
MCH (pg), median [IQR]	30.3 [29.5; 31.2]	30.5 [29.2; 31.4]	0.917
MCHC (g/L), median [IQR]	338 [330; 348]	338 [328; 345]	0.311
RDW (%), median [IQR]	13.0 [12.5; 13.7]	12.9 [12.2; 13.6]	0.186
Platelet count (*10 ⁹ /L), median [IQR]	196 [158; 227]	206 [171; 249]	0.082
Platelet distribution width (%), median [IQR]	13.9 [12.2; 15.8]	12.7 [11.1; 14.3]	<0.001
Prothrombin time (seconds), median [IQR]	13.4 [13.0; 13.9]	13.3 [12.9; 13.8]	0.060
Activated partial thromboplastin time (seconds), median [IQR]	34.2 [32.0; 36.8]	34.5 [32.2; 37.2]	0.434
International normalized ratio, median [IQR]	1.03 [1.00; 1.08]	1.02 [0.97; 1.06]	0.020
Total cholesterol (seconds), median [IQR]	4.27 [3.65; 5.04]	4.33 [3.70; 4.94]	0.806
Serum glucose (mmol/L), median [IQR]	6.72 [5.56; 8.43]	6.84 [5.80; 8.33]	0.640
Time from first NCCT scan to onset (hours), median [IQR]	3.00 [1.88; 4.12]	3.00 [1.50; 4.00]	0.472
Radiological characteristics			
Hematoma location (%):			<0.001
Thalamus	28 (21.2)	43 (17.4)	
Basal ganglia	101 (76.5)	157 (63.6)	
Brain stem or cerebella	0 (0.0)	11 (4.5)	
Cerebral lobe	3 (2.3)	36 (14.6)	
Baseline hematoma volume (ml), median [IQR]	19.6 [9.25; 34.7]	16.8 [8.69; 30.6]	0.187
Largest hematoma width/length ratio on axial section (>0.6), (%)	65 (49.2)	119 (48.2)	0.929
Midline shift distance (>0.5 cm), (%)	41 (31.1)	51 (20.6)	0.033
Subarachnoid hemorrhage (%)	7 (5.30)	15 (6.07)	0.940
Intraventricular hemorrhage (%)	48 (36.4)	62 (25.1)	0.029
Swirl sign (%)	19 (14.4)	44 (17.8)	0.479
Black hole sign (%)	10 (7.58)	26 (10.5)	0.454
Blend sign (%)	12 (9.1)	49 (19.8)	0.011
Irregular sign (%)	51 (38.6)	95 (38.5)	1.000
Satellite sign (%)	39 (29.5)	68 (27.5)	0.768

(Continued)

TABLE 1 | Continued

Variables	Derivation cohort (n = 132)	Validation cohort (n = 247)	P
Island sign (%)	13 (9.85)	23 (9.31)	1.000
Attenuation value of non-hypodense region (HU), median [IQR]	66.2 [63.1; 69.3]	67.6 [64.4; 70.8]	0.011
Outcome			
HE (%)	31 (23.5%)	72 (29.1%)	0.289
3 months mRS score (4~6), (%)	60 (45.5%)	128 (51.8%)	0.283

SD, standard deviation; IQR, interquartile range; GCS, Glasgow coma scale; RBC, red blood cell; MCV, mean corpuscular volume; MCH, mean corpuscular hemoglobin; MCHC, mean corpuscular hemoglobin concentration; RDW, red blood cell distribution width; NCCT, non-contrast CT; HU, Hounsfield units; HE, hematoma expansion; mRS, modified Rankin scale.

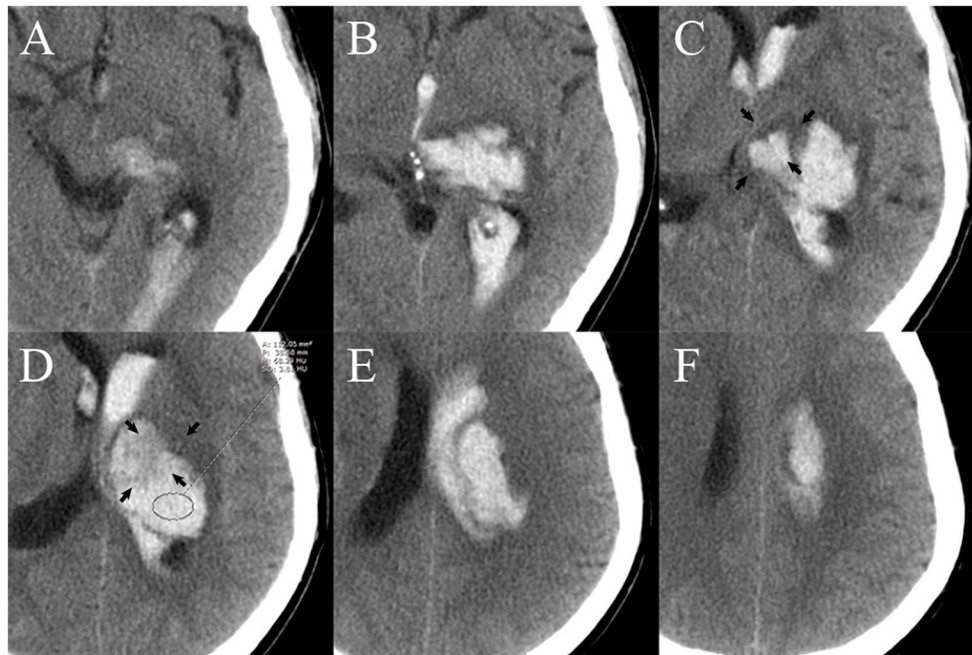


FIGURE 2 | Measurement of the attenuation value of the region of interest (ROI) of the non-hyperdense region of the hematoma. There are six layers of hematoma on axial NCCT images. The upper (A,B) and lower layers (E,F) are not suitable for measurement because they are adjacent to normal brain tissue. The core two layers (C,D) are selected as the best layer for measurement. The area of layer (D) (black arrow) that is adjacent to normal tissue [layer (C), black arrow] may cause partial volume effects that affect the accuracy of the measurement and is therefore excluded from the ROI. A, area; P, perimeter; M, mean; SD, standard deviation; HU, Hounsfield units; NCCT, non-contrast computed tomography.

no significant correlation between the attenuation value within the non-hypodense region of the hematoma and the time from the first NCCT scan to onset, irrespective of the occurrence of HE (Figure 4A). NCCT attenuation value was generally lower within the non-hypodense region of expanded hematomas, and this difference was more pronounced in the brainstem or cerebellar locations (Figure 4B). A positive correlation existed between attenuation value within the non-hypodense region and hemoglobin level (Figure 4C), and a negative correlation existed referring to the red blood cell distribution width, regardless of whether the hematoma was expanded (Figure 4D).

Derivation of the Critical Attenuation Value of Hematoma to Predict HE

An ROC curve analysis showed that the cutoff of attenuation value within non-hypodense region for predicting HE was <64 HU, and its sensitivity, specificity, PLR, NLR, PPV, NPV,

and AUC were 67.74% (95% CI, 48.6–83.3%), 82.18% (95% CI, 73.3–89.1%), 3.8 (95% CI, 2.3–6.2), 0.39 (95% CI, 0.2–0.7), 53.8% (95% CI, 41.8–65.4%), 89.2% (95% CI, 83.2–93.3%), and 0.722 (95% CI, 0.600–0.844, $p < 0.001$), indicating its suitability for predicting HE (Figure 5A). A total of 40 hematomas had an attenuation value of <64 HU within the non-hypodense region and there were 31 heterogeneous hematomas. Among them, 8 of 9 hematomas with regular morphology and homogeneous density and suffered HE, and had a density value of < 64 HU ($p < 0.001$). Seven of the 11 patients with irregular morphology, homogeneous density, and dilatation had an attenuation value < 64 HU ($p = 0.028$). Among the heterogeneous hematomas, 6 of the 9 hematomas with a non-hypodense region attenuation value of <64 HU and only 5 of the 22 hematomas with a non-hypodense region attenuation value of >64 HU that eventually expanded ($p = 0.02$).

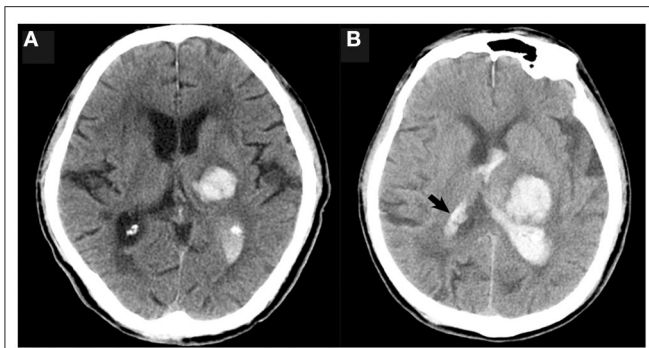


FIGURE 3 | The initial NCCT showed that the thalamic hematoma broke into the ipsilateral ventricle only (A); a follow-up NCCT (B) showed new hematoma formation in both the ipsilateral and contralateral ventricles (black arrow).

Validation of the Association Between Attenuation Value < 64 HU and HE

There was good inter-rater (rater 1, $\kappa = 0.967$; rater 2, $\kappa = 0.956$) and intra-rater ($\kappa = 0.945$, rater 1 vs. rater 2) agreement for the measurement of attenuation value <64 HU. A univariate logistic analysis showed that attenuation value within non-hypodense region <64 HU was associated with HE, both unadjusted and after adjusting for other factors (Table 2). An ROC analysis showed that the sensitivity, specificity, PLR, NLR, PPV, NPV, and AUC of the attenuation value <64 HU for HE prediction were 36.11% (95% CI, 25.1–48.3%), 81.71% (95% CI, 75.2–87.1%), 1.97 (95% CI, 1.3–3.1), 0.78 (95% CI, 0.6–0.9), 44.8% (95% CI, 34.4–55.8%), 75.7% (95% CI, 72.0–78.9%), and 0.589 (95% CI, 0.526–0.652, $p = 0.005$) (Figure 5B). There were 89 heterogeneous hematomas and there were 58 hematomas that had attenuation value < 64 HU within the non-hypodense region. Of the 14 hematomas with regular morphology, homogenous density and subsequent expansion, 9 had attenuation value <64 HU ($p < 0.001$). Out of 22 patients with irregular morphology, homogeneous density and who underwent expansion, 11 had attenuation value <64 HU ($p = 0.041$). Among heterogeneous hematomas, expansion occurred in the 6 of 12 hematomas with attenuation value <64 HU in the non-hypodense region and in 30 of 77 hematomas with attenuation value >64 HU in the non-hypodense region of the hematoma ($p = 0.683$).

A LASSO analysis was applied to screen for predictors without the collinearity of HE (Figures 6A,B). The multivariate model showed that an attenuation value < 64 HU remained an independent predictor [odds ratio (OR), 4.118; 95% CI, 1.897–9.129, $p < 0.001$] after adjusting for male sex, time from the first NCCT scan to onset, baseline hematoma volume, blend sign, and irregular sign (Figure 6C, Supplementary Table 1).

Based on the multivariate model, the nomogram was constructed (Figure 7A) and its discriminating and calibrating ability was favorable with a C-index/AUC of 0.806 (Supplementary Figure 3) and good calibration (Figure 7B). In addition, the model showed good discrimination ability in derivation cohort and combined cohorts with the C-indexes of 0.883 and 0.823. A decision curve analysis showed that an

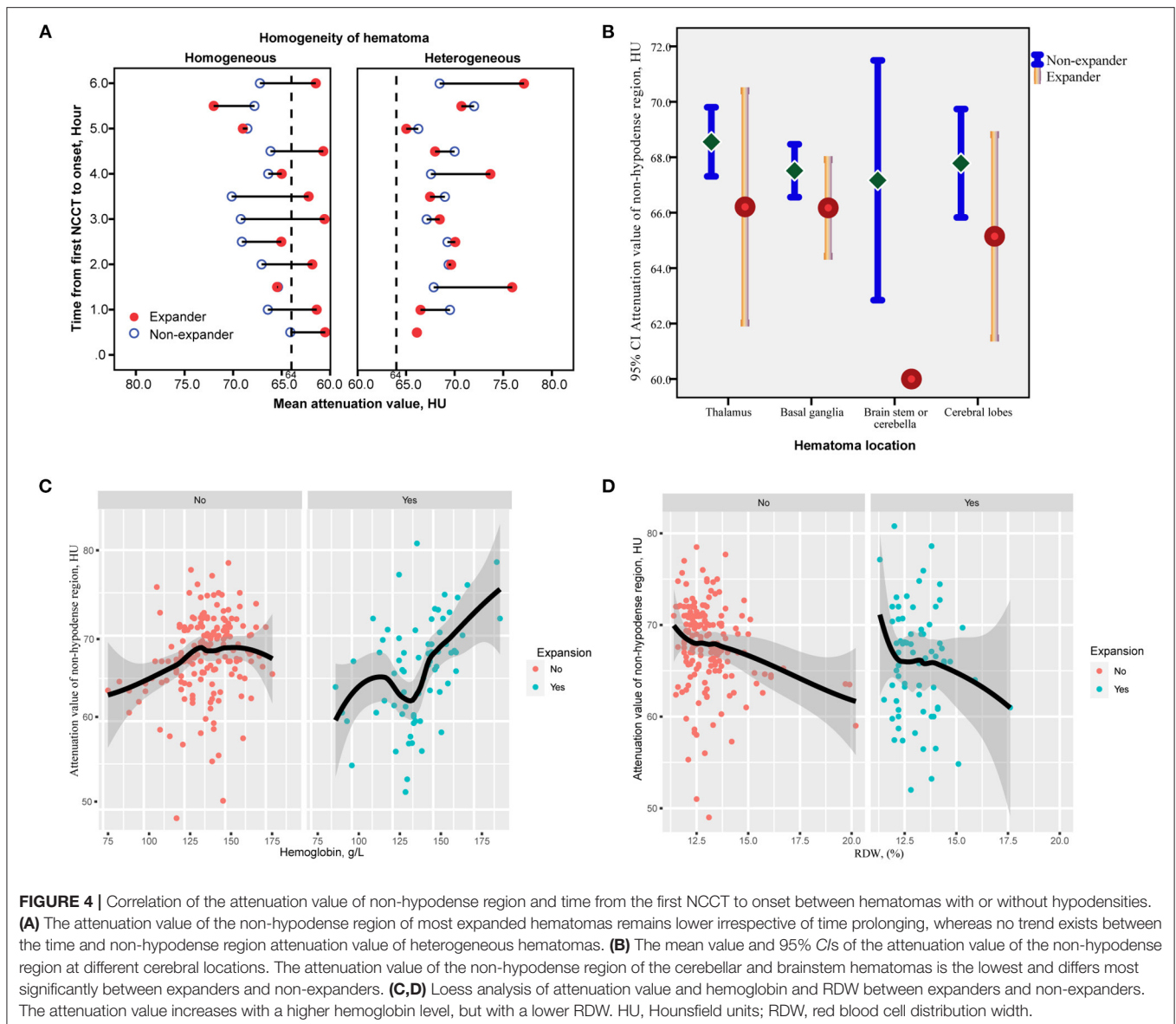
attenuation value < 64 HU significantly improved the predicted net benefit when the probability of HE varied in the range of ~0.3–0.6 (Figure 7C). The clinical impact curve showed that the predicted and actual number of HE was close when the threshold risk of HE exceeded ~0.5 (Figure 7D).

DISCUSSION

The attenuation value of intracerebral hematoma on the NCCT is one of the indicators that have received much attention in recent years for it can be used to predict HE which seriously affects the prognosis of a patient (14–16). Studies had shown that the difference of attenuation value between high-density and low-density areas that had a clear margin within hematoma >18 HU (7, 17–19), and the minimal attenuation value of the hematoma ≤ 31 HU were independent risk factors for predicting HE (20). Here, according to our study, the attenuation value within the non-hypodense region of the hematoma is also an independent predictor associated with HE, and an attenuation value <64 HU is a potential cutoff.

There is no doubt that the hemostatic status of the bleeding site of the ruptured vessel is the fundamental cause of whether the hematoma will enlarge. In the early stages of intracerebral hemorrhage, the density of fresh hematoma is ~+30 to 45 HU (21). Then, it gradually increases during the initial ~48 h and then decreases again after reaching the peak value (5, 22, 23). The increased attenuation value of the hematoma is mainly due to the formation of a meshwork of fibrin fibers, globin molecules, and early clot contraction events after bleeding (5, 24), therefore hypodense foci within the hematoma may be the result of repeated bleeding from the primary bleeding site or poor clot contraction and hence the evidence of the potential HE (7, 9, 17). However, the exact site of hemorrhage, whether it is a primary hemorrhagic vessel (25), or a secondary hemorrhagic vessel (26), is not always within the hypodense foci, but may also be located within the non-hypodense region and appear as a spot sign on contrast CT (6, 27). Therefore, the role played by the attenuation value within the non-hypodense region in determining the hemostatic status of the bleeding site is not negligible.

The attenuation value of the hyperdense area of hematoma has been taken into account sparsely in assessing the probability of HE. In the acquirement of the mean attenuation value of hematoma by Jeong et al., both the hypodense and non-hypodense regions of hematoma were measured in a *post-hoc* analysis, though the mean density of the hematoma with and without hypodense foci was not statistically significant, the mean density of the dilated hematoma was significantly lower (5). Nevertheless, their study failed to account for the proportion of high-density and low-density regions in each hematoma, so the unique role of the non-hypodense regions in hematoma expansion cannot be accurately determined. In contrast, our study confirmed that the non-hypodense regions of the expanded hematoma do possess a lower attenuation value. To the best of our knowledge, there is no clearly reported indicator regarding NCCT hematoma density that can be used as a predictor of secondary expansion of homogeneous hematomas. Since the existing hypodensity sign,



swirl sign, black hole sign, and blend sign are based on hypodense regions to determine the risk of HE, the attenuation value within the non-hypodense region of the hematoma provides an option to determine whether a homogeneous hematoma is at high risk. In addition, heterogeneous hematomas with this feature may have a greater likelihood of expansion. This feature does not intersect with the hematoma morphology and low-density markers that predict HE, and quantifies the density values of the high-density areas independently of the low-density areas within the hematoma, avoiding the influence of the proportion of low-density areas in the calculation of mean density value and thus having independent diagnostic value.

The multifactor model incorporated predictors involving the attenuation value level within the non-hypodense region that was determined by LASSO regression and was presented in the form of a nomogram, allowing for a clearer understanding of

the role played by each predictor. The nomogram is simple and feasible, applicable to individual patients and practitioners in daily clinical practice, and the data are easily accessible (28, 29). The discriminative power of our model is good compared with previous reports (29, 30), with a cutoff nomogram score of about 126 and a corresponding prevalence of about 0.3 of expansion, the patient has a high probability of HE. A decision curve analysis can be used to visually and graphically evaluate the ability of each component to improve the model and has been highly recommended in recent years (31, 32). Our model shows that the net benefit of treatment is higher when the risk of hematoma varies between 0.3 and 0.6, thus taking into account the magnitude of the attenuation value within the non-hypodense region may be more helpful (Net Reclassification Improvement = 0.4336, $p = 0.001$; Integrated Discrimination Improvement = 0.0483, $p = 0.002$) in making

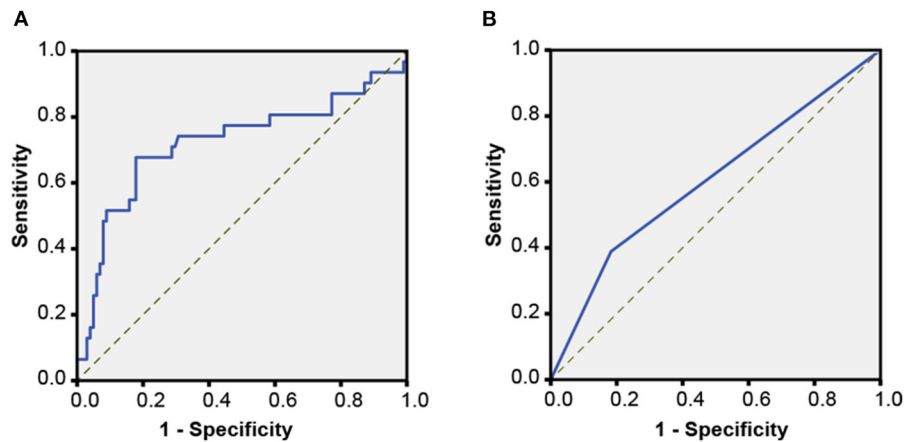


FIGURE 5 | Receiver operating characteristic (ROC) curves. **(A)** An ROC analysis for determining the critical attenuation value of the non-hypodense region of hematoma in the derivation cohort. **(B)** An ROC analysis of the attenuation value <64 HU for predicting HE in the validation cohort.

TABLE 2 | Variables with statistical significance for predicting HE analyzed by univariate logistic regression.

Variables	Crude			Model 1			Model 2			Model 3		
	OR	95% CI	P	OR	95% CI	P	OR	95% CI	P	OR	95% CI	P
Sex, male	2.056	1.103–3.834	0.023	2.033	1.028–4.022	0.041	2.235	0.948–5.272	0.066	3.140	1.129–8.734	0.028
Time from first NCCT scan to onset, hour	0.764	0.632–0.925	0.006	0.751	0.618–0.914	0.004	0.673	0.532–0.850	0.001	0.611	0.462–0.809	0.001
Baseline GCS score	1.562	1.100–2.219	0.013	1.644	1.140–2.373	0.008	1.470	0.966–2.236	0.072	1.297	0.762–2.208	0.338
Baseline hematoma volume, ml	1.023	1.010–1.037	0.001	1.024	1.011–1.038	<0.001	1.022	1.006–1.038	0.008	1.014	0.993–1.037	0.200
Blend sign	2.980	1.559–5.695	0.001	2.860	1.462–5.595	0.002	3.916	1.793–8.552	0.001	3.471	1.326–9.038	0.011
Irregular sign	3.223	1.825–5.691	<0.001	3.578	1.957–6.540	<0.001	3.554	1.739–7.263	0.001	2.911	1.021–8.304	0.046
Island sign	1.727	1.118–2.668	0.014	1.948	1.219–3.115	0.005	2.227	1.303–3.808	0.003	2.079	0.954–4.527	0.065
Attenuation value of non-hypodense region, HU	0.935	0.886–0.986	0.014	0.926	0.876–0.979	0.007	0.912	0.854–0.974	0.006	0.845	0.770–0.928	<0.001
Attenuation value of non-hypodense region <64 HU	2.140	1.111–4.122	0.023	3.072	1.577–5.986	0.001	4.337	1.885–9.978	0.001	10.252	3.306–31.788	<0.001

Variables that were statistically significant in the univariate analysis were adjusted again to observe whether there was a significant change of OR for the coexistence of other factors. Model 1: Adjusted for age, sex, co-existing diseases (hypertension, diabetes, current smoker, current alcohol drinker, and stroke history), and antiplatelets or anticoagulants therapy. Model 2: Adjusted for Model 1, physical examination results (systolic pressure, diastolic pressure, and baseline GCS score) and laboratory findings (RBC count, hemoglobin, hematocrit, MCV, MCH, MCHC, RDW, platelet count, platelet distribution width, prothrombin time, activated partial thromboplastin time, international normalized ratio, total cholesterol, and serum glucose). Model 3: Adjusted for Model 2, time from the first NCCT scan to onset, and hematoma features on NCCT scan (location, baseline hematoma volume, hematoma width/length ratio on axial section, midline shift distance > 0.5 cm, subarachnoid hemorrhage, intraventricular hemorrhage, swirl sign, black hole sign, blend sign, irregular sign, satellite sign, and island sign). HE, hematoma expansion; OR, odds ratio; CI, Confidence interval; NCCT, non-contrast CT; GCS, Glasgow coma scale; HU, Hounsfield units; RBC, red blood count; MCV, mean corpuscular volume; MCH, mean corpuscular hemoglobin; MCHC, mean corpuscular hemoglobin concentration; RDW, RBC distribution width.

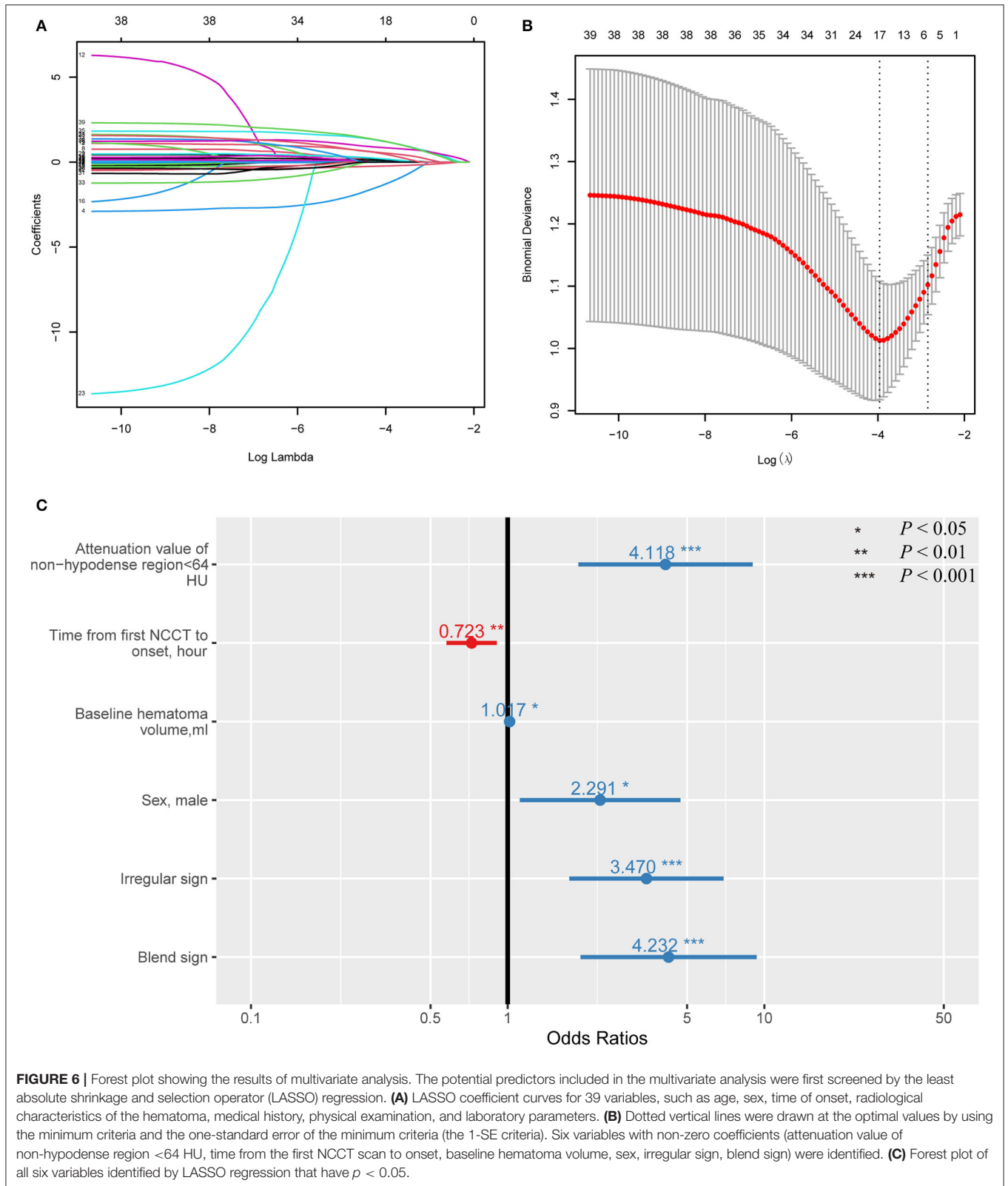
the right clinical decisions when the risk of HE determined by assessment methods is within this range. Besides, the prediction will be more accurate if the threshold of HE is >0.5 according to the clinical impact curve.

The study has some limitations. First, the relatively small number of subjects may have produced some selective bias. In addition, the attenuation of the non-hypodense region was not suitable for predicting intracerebral hematomas with volume <1 ml, which means that most hematomas located in the midbrain, pons, and medulla may not be applicable. The study also excluded multiple intracerebral hemorrhages, although some of these hematomas may have the same etiology, the non-hypodense region attenuation value, and associated model may not be suitable for these hematomas. Again, although the model

performed well in our dataset, a follow-up replication study is necessary to validate it as the new metric that has not been studied in other literature. Finally, the optimal cutoff of the new predictor may need to be modified to reach higher accuracy.

CONCLUSIONS

In conclusion, our study explored and validated the attenuation value of the non-hypodense region of hematoma that was independently associated with early HE in patients with spontaneous cerebral hemorrhage. The critical attenuation value < 64 HU was shown to be an appropriate indicator of possible subsequent HE and was able to significantly improve the predictive power of the multifactor model.



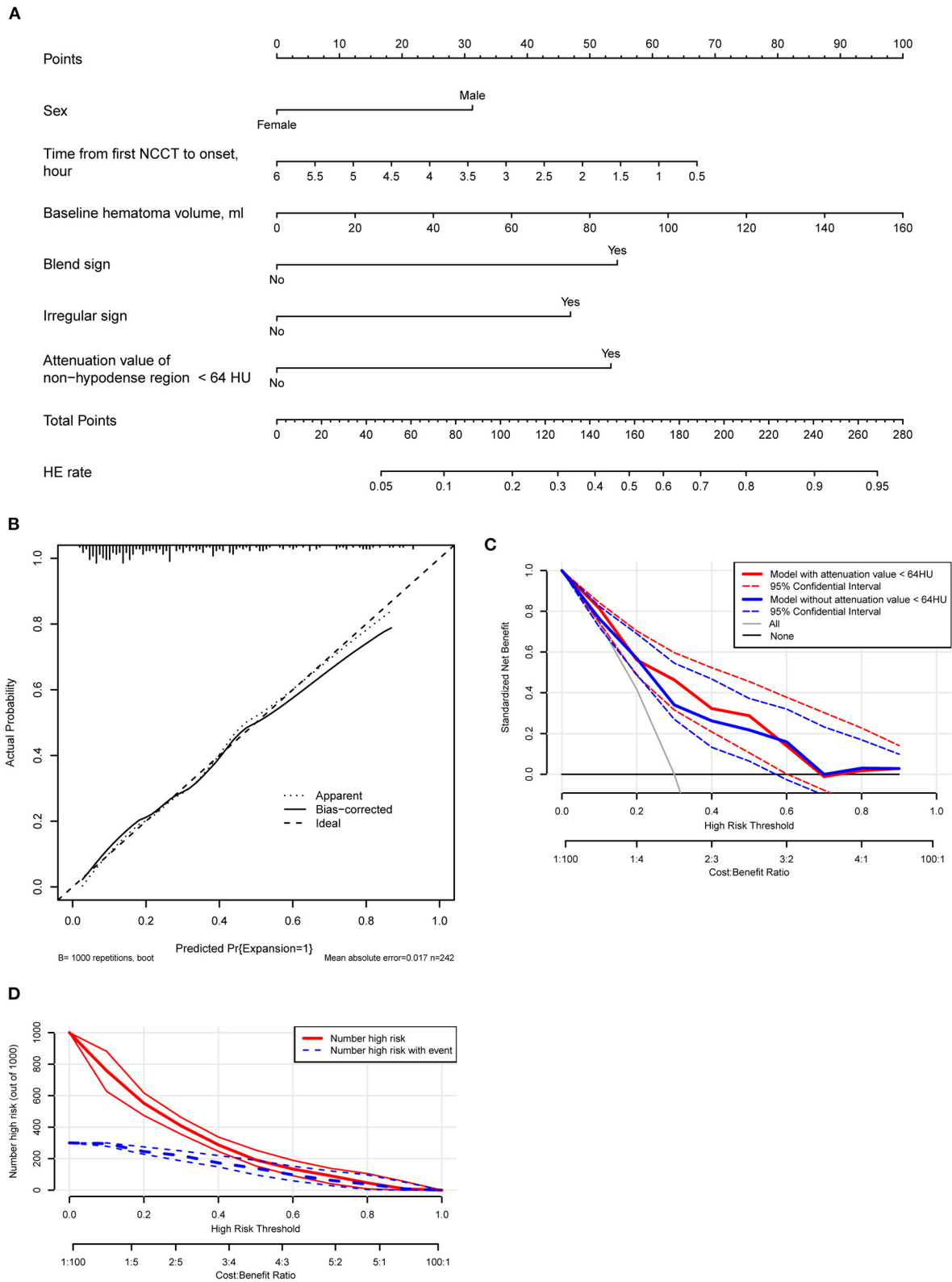


FIGURE 7 | (A) A nomogram is derived from the multivariate analysis. **(B)** Calibration plot of the nomogram model. **(C)** A decision curve analysis of the model with or without incorporation of the attenuation value of the non-hypodense region of hematoma. The model with six variables has a higher net benefit when the expansion risk threshold varies between 0.3 and 0.6. **(D)** Clinical impact curve analysis. The actual events and the predicted events are close while the risk of threshold exceeds about 0.5.

DATA AVAILABILITY STATEMENT

The raw data supporting the conclusions of this article will be made available on request to the corresponding author, without undue reservation.

ETHICS STATEMENT

The studies involving human participants were reviewed and approved by Ethics Committee of Tongji Hospital, Huazhong University of Science and Technology. Written informed consent for participation was not required for this study in accordance with the national legislation and the institutional requirements.

AUTHOR CONTRIBUTIONS

YC contributed to the study conception and design. Material preparation, data collection, and analysis were performed by YC, DC, X-LM, and Z-QG. The first draft of the manuscript was written by YC and reviewed by Y-BO, YH, XC, and JC. All authors commented on previous versions of the manuscript. All authors read and approved the final manuscript.

REFERENCES

- Davis SM, Broderick J, Hennerici M, Brun NC, Diringer MN, Mayer SA, et al. Hematoma growth is a determinant of mortality and poor outcome after intracerebral hemorrhage. *Neurology*. (2006) 66:1175–81. doi: 10.1212/01.wnl.0000208408.98482.99
- Mayer SA, Davis SM, Skolnick BE, Brun NC, Begtrup K, Broderick JP, et al. Can a subset of intracerebral hemorrhage patients benefit from hemostatic therapy with recombinant activated factor VII? *Stroke*. (2009) 40:833–40. doi: 10.1161/STROKEAHA.108.524470
- Gladstone DJ, Aviv RI, Demchuk AM, Hill MD, Thorpe KE, Khoury JC, et al. Effect of recombinant activated coagulation factor vii on hemorrhage expansion among patients with spot sign-positive acute intracerebral hemorrhage: the SPOTLIGHT and STOP-IT randomized clinical trials. *JAMA Neurol*. (2019) 76:1493–501. doi: 10.1001/jamaneuro.2019.2636
- Hussein O, Sawalha K, Fritz J, Abd Elazim A, Hamed M, Wei L, et al. The significance of contrast density of the computed tomography-angiographic spot sign and its correlation with hematoma expansion. *J Stroke Cerebrovasc Dis*. (2019) 28:1474–82. doi: 10.1016/j.jstrokecerebrovasdis.2019.03.020
- Jeong HG, Bang JS, Kim BJ, Bae HJ, Han MK. Hematoma Hounsfield units and expansion of intracerebral hemorrhage: a potential marker of hemostatic clot contraction. *Int J Stroke*. (2021) 16:163–71. doi: 10.1177/1747493019895703
- Sporns PB, Schwake M, Kemmling A, Minnerup J, Schwindt W, Niederstadt T, et al. Comparison of spot sign, blend sign and black hole sign for outcome prediction in patients with intracerebral hemorrhage. *J Stroke*. (2017) 19:333–9. doi: 10.5853/jos.2016.02061
- Li Q, Zhang G, Huang YJ, Dong MX, Lv FJ, Wei X, et al. Blend sign on computed tomography: novel and reliable predictor for early hematoma growth in patients with intracerebral hemorrhage. *Stroke*. (2015) 46:2119–23. doi: 10.1161/STROKEAHA.115.009185
- Boulouis G, Morotti A, Brouwers HB, Charidimou A, Jessel MJ, Auriel E, et al. Association between hypodensities detected by computed tomography and hematoma expansion in patients with intracerebral hemorrhage. *JAMA Neurol*. (2016) 73:961–8. doi: 10.1001/jamaneuro.2016.1218
- Li Q, Zhang G, Xiong X, Wang XC, Yang WS, Li KW, et al. Black hole sign: novel imaging marker that predicts hematoma growth in patients with intracerebral hemorrhage. *Stroke*. (2016) 47:1777–81. doi: 10.1161/STROKEAHA.116.013186
- Yang X, Zhu Y, Zhang L, Wang L, Mao Y, Li Y, et al. The initial CT blend sign is not associated with poor patient outcomes after stereotactic minimally invasive surgery. *BMC Neurol*. (2021) 21:160. doi: 10.1186/s12883-021-02181-0
- Morotti A, Boulouis G, Dowlatshahi D, Li Q, Barras CD, Delcourt C, et al. Standards for detecting, interpreting, and reporting noncontrast computed tomographic markers of intracerebral hemorrhage expansion. *Ann Neurol*. (2019) 86:480–92. doi: 10.1002/ana.25563
- Yogendrakumar V, Ramsay T, Fergusson DA, Demchuk AM, Aviv RI, Rodriguez-Luna D, et al. Redefining hematoma expansion with the inclusion of intraventricular hemorrhage growth. *Stroke*. (2020) 51:1120–7. doi: 10.1161/STROKEAHA.119.027451
- Sauerbrey W, Royston P, Binder H. Selection of important variables and determination of functional form for continuous predictors in multivariable model building. *Stat Med*. (2007) 26:5512–28. doi: 10.1002/sim.3148
- Barras CD, Tress BM, Christensen S, Collins M, Desmond PM, Skolnick BE, et al. Quantitative CT densitometry for predicting intracerebral hemorrhage growth. *AJNR Am J Neuroradiol*. (2013) 34:1139–44. doi: 10.3174/ajnr.A3375
- Law ZK, Ali A, Krishnan K, Bischoff A, Appleton JP, Scutt P, et al. Noncontrast computed tomography signs as predictors of hematoma expansion, clinical outcome, and response to tranexamic acid in acute intracerebral hemorrhage. *Stroke*. (2020) 51:121–8. doi: 10.1161/STROKEAHA.119.026128
- Morotti A, Arba F, Boulouis G, Charidimou A. Noncontrast CT markers of intracerebral hemorrhage expansion and poor outcome: a meta-analysis. *Neurology*. (2020) 95:632–43. doi: 10.1212/WNL.00000000000010660
- Ng D, Churilov L, Mitchell P, Dowling R, Yan B. The CT Swirl sign is associated with hematoma expansion in intracerebral hemorrhage. *AJNR Am J Neuroradiol*. (2018) 39:232–7. doi: 10.3174/ajnr.A5465
- Zhang D, Chen J, Guo J, Jiang Y, Dong Y, Ping-Chi Chen B, et al. Hematoma heterogeneity on noncontrast computed tomography predicts intracerebral hematoma expansion: a meta-analysis. *World Neurosurg*. (2018) 114:e663–76. doi: 10.1016/j.wneu.2018.03.048
- Chen Y, Tian L, Wang L, Qin Y, Cai J. Black hole sign on noncontrast computed tomography in predicting hematoma expansion in patients with

SUPPLEMENTARY MATERIAL

The Supplementary Material for this article can be found online at: <https://www.frontiersin.org/articles/10.3389/fneur.2022.785670/full#supplementary-material>

Supplementary Figure 1 | Flowchart for the patient selection of two patient cohorts.

Supplementary Figure 2 | Correlation heatmap of the potential predictors (continuous variables) of hematoma expansion (HE). The hemoglobin, hematocrit, and MCHC are the positively related factor of HU, whereas the RDW is the negatively related factor that with statistical significance. SBP, systolic pressure; DBP, diastolic pressure; RBC, red blood cell; Hb, hemoglobin; HCT, hematocrit; MCV, mean corpuscular volume; MCH, mean corpuscular hemoglobin; MCHC, mean corpuscular hemoglobin concentration; RDW, RBC distribution width; PLT, platelet; PDW, platelet distribution width; PT, prothrombin time; APTT, activated partial thromboplastin time; INR, international normalized ratio; TC, total cholesterol; SG, serum glucose; BV, baseline hematoma volume; HU, Hounsfield units.

Supplementary Figure 3 | The receiver operating characteristic (ROC) analysis of the multivariate model. The C-index/area under the curve (AUC) is 0.806. The corresponding nomogram score for cutoff is 126 (asterisk).

Supplementary Table 1 | Multivariate analysis of the predictors of HE identified by LASSO regression.

- intracerebral hemorrhage: a meta-analysis. *Curr Med Imaging.* (2020) 16:878–86. doi: 10.2174/1573405615666190903155738
20. Chu H, Huang C, Dong J, Yang X, Xiang J, Mao Y, et al. Minimal computed tomography attenuation value within the hematoma is associated with hematoma expansion and poor outcome in intracerebral hemorrhage patients. *Neurocrit Care.* (2019) 31:455–65. doi: 10.1007/s12028-019-00754-z
 21. DenOtter TD, Schubert J. *Hounsfield Unit. StatPearls.* Treasure Island, FL: StatPearls Publishing LLC (2021).
 22. Bergström M, Ericson K, Levander B, Svendsen P, Larsson S. Variation with time of the attenuation values of intracranial hematomas. *J Comput Assist Tomogr.* (1977) 1:57–63. doi: 10.1097/00004728-197701000-00008
 23. Parizel PM, Makkat S, Van Miert E, Van Goethem JW, van den Hauwe L, De Schepper AM. Intracranial hemorrhage: principles of CT and MRI interpretation. *Eur Radiol.* (2001) 11:1770–83. doi: 10.1007/s003300000800
 24. Cines DB, Lebedeva T, Nagaswami C, Hayes V, Massefski W, Litvinov RI, et al. Clot contraction: compression of erythrocytes into tightly packed polyhedra and redistribution of platelets and fibrin. *Blood.* (2014) 123:1596–603. doi: 10.1182/blood-2013-08-523860
 25. Cao D, Li Q, Fu P, Zhang J, Yang J. Early Hematoma Enlargement in Primary Intracerebral Hemorrhage. *Curr Drug Targets.* (2017) 18:1345–8. doi: 10.2174/1389450118666170427151011
 26. Fisher CM. Pathological observations in hypertensive cerebral hemorrhage. *J Neuropathol Exp Neurol.* (1971) 30:536–50. doi: 10.1097/00005072-197107000-00015
 27. Zheng J, Yu Z, Xu Z, Li M, Wang X, Lin S, et al. The accuracy of the spot sign and the blend sign for predicting hematoma expansion in patients with spontaneous intracerebral hemorrhage. *Med Sci Monit.* (2017) 23:2250–7. doi: 10.12659/MSM.901583
 28. Yang M, Du C, Zhang Q, Ma Q, Li R. Nomogram model for predicting hematoma expansion in spontaneous intracerebral hemorrhage: multicenter retrospective study. *World Neurosurg.* (2020) 137:e470–8. doi: 10.1016/j.wneu.2020.02.004
 29. Zhang C, Ge H, Zhong J, Yin Y, Fang X, Zou Y, et al. Development and validation of a nomogram for predicting hematoma expansion in intracerebral hemorrhage. *J Clin Neurosci.* (2020) 82:99–104. doi: 10.1016/j.jocn.2020.10.027
 30. Chen Q, Zhu D, Liu J, Zhang M, Xu H, Xiang Y, et al. Clinical-radiomics nomogram for risk estimation of early hematoma expansion after acute intracerebral hemorrhage. *Acad Radiol.* (2021) 28:307–17. doi: 10.1016/j.acra.2020.02.021
 31. Vickers AJ, Elkin EB. Decision curve analysis: a novel method for evaluating prediction models. *Med Decis Making.* (2006) 26:565–74. doi: 10.1177/0272989X06295361
 32. Rousson V, Zumbo T. Decision curve analysis revisited: overall net benefit, relationships to ROC curve analysis, and application to case-control studies. *BMC Med Inform Decis Mak.* (2011) 11:45. doi: 10.1186/1472-6947-11-45

Conflict of Interest: The authors declare that the research was conducted in the absence of any commercial or financial relationships that could be construed as a potential conflict of interest.

Publisher's Note: All claims expressed in this article are solely those of the authors and do not necessarily represent those of their affiliated organizations, or those of the publisher, the editors and the reviewers. Any product that may be evaluated in this article, or claim that may be made by its manufacturer, is not guaranteed or endorsed by the publisher.

Copyright © 2022 Chen, Cao, Guo, Ma, Ou, He, Chen and Chen. This is an open-access article distributed under the terms of the Creative Commons Attribution License (CC BY). The use, distribution or reproduction in other forums is permitted, provided the original author(s) and the copyright owner(s) are credited and that the original publication in this journal is cited, in accordance with accepted academic practice. No use, distribution or reproduction is permitted which does not comply with these terms.